

RESEARCH PAPER

Identification of auxins by a chemical genomics approach

May Christian¹, William B. Hannah¹, Hartwig Lüthen² and Alan M. Jones^{1,*}

¹ Departments of Biology and Pharmacology, The University of North Carolina at Chapel Hill, NC 27599-3280, USA

² Biozentrum Klein Flottbek und Botanischer Garten, Ohnhorststrasse 18, 22609 Hamburg, Germany

Received 7 February 2008; Revised 31 March 2008; Accepted 14 April 2008

Abstract

Thirteen auxenic compounds were discovered in a screen of 10 000 compounds for auxin-like activity in *Arabidopsis* roots. One of the most potent substances was 2-(4-chloro-2-methylphenoxy)-N-(4-H-1,2,4-triazol-3-yl)acetamide (WH7) which shares similar structure to the known auxenic herbicide 2,4-dichlorophenoxyacetic acid (2,4-D). A selected set of 20 analogues of WH7 was used to provide detailed information about the structure–activity relationship based on their efficacy at inhibiting and stimulating root and shoot growth, respectively, and at induction of gene expression. It was shown that WH7 acts in a genetically defined auxin pathway. These small molecules will extend the arsenal of substances that can be used to define auxin perception site(s) and to dissect subsequent signalling events.

Key words: Auxin, 2,4-D, growth control, sensitivity, structure–activity.

Introduction

Auxins regulate plant cell elongation and division (Evans, 1984; Chen *et al.*, 2001b; Christian *et al.*, 2006). The natural auxin, indole-3-acetic acid (IAA), is ubiquitously distributed, but target cell responsiveness varies between organs and developmental stages. The underlying mechanisms of perception and signal transduction are still a matter of debate.

Auxin binding protein 1 (ABP1) is an auxin receptor (Hertel *et al.*, 1972) that is ubiquitous throughout tissues but highest in regions that are expanding and maintain high capacity of auxin-inducible growth (Harnden and Jones, 1995). At the subcellular level, ABP1 is predominantly localized in the endoplasmic reticulum but

≥2% of the ABP1 pool is secreted (Jones and Herman, 1993; Diekmann *et al.*, 1995; Tian *et al.*, 1995; Henderson *et al.*, 1997). Unlike other external sensors, the protein sequence of ABP1 reveals no membrane-spanning domains. Therefore, a transmembrane docking-protein was proposed, placing ABP1 into an extracellular, auxin-dependent complex (Klämbt, 1990; MacDonald, 1997).

While a large body of evidence supports a role for ABP1 in a subset of auxin responses (Barbier-Brygoo *et al.*, 1991; Jones *et al.*, 1998; Chen *et al.*, 2001a, b; Steffens *et al.*, 2001; Christian *et al.*, 2003), the entire spectrum of auxin action on the cell is not encompassed by ABP1 action; there are other auxin sensors (Hertel, 1995; Claussen *et al.*, 1996; Kim *et al.*, 2001; Yamagami *et al.*, 2004; Walsh *et al.*, 2006). The auxin signalling F-box protein (AFB) family, a group of F-box proteins comprising E3 ligases, is involved in the degradation of auxin response repressors (Aux/IAAs) and therefore indirectly the modulation of gene expression (Dharmasiri *et al.*, 2005; Kepinski and Leyser, 2005). Kepinsky and Leyser (2005) showed that IAA and the synthetic auxins 2,4-D and 1-naphthaleneacetic acid (1-NAA) increase the association of TIR1, the prototype of the AFB-family, to at least one of its protein targets. Dharmasiri *et al.* (2005) generated loss-of-function mutants and demonstrated that successive loss of TIR1 and related F-box proteins increasingly eliminates auxin-responsiveness. The crystal structure of ligand-bound and ligand-free TIR1 revealed that auxin functions as a ‘molecular-glue’ between TIR1 and its substrate, rather than modifying either protein (Tan *et al.*, 2007). The task at hand is to perform careful characterizations of those sensors in order to dissect which auxin responses each mediates. Toward this end, forward chemical genomics (MacBeath, 2001) has become an important tool. The approach combines identification of bioactive chemicals with genetic screens (Armstrong *et al.*, 2004; Lipinski and Hopkins, 2004; Surpin *et al.*,

* To whom correspondence should be addressed. E-mail: alan_jones@unc.edu

2005; Walsh *et al.*, 2006) and has become possible due to advances in combinatorial chemistries (reviewed in Raikhel and Pirrung, 2005).

Here the identification of auxins from a chemical screen of a combinatorial chemical library of 10 000 compounds is described. These auxins represent new tools to dissect auxin receptor action.

Materials and methods

Plant materials and growth conditions

All *Arabidopsis thaliana* mutant and transgenic lines used in this study were in the Columbia background (Col-0). *Arabidopsis* wild-type seeds were sterilized and sown on 1× or 0.5× Murashige–Skoog (MS) media (Invitrogen, San Diego, CA, USA) containing 0.8% or 0.6% phytagar (Invitrogen).

Chemical library screen

The primary screen was performed at the University of California at Riverside using a library containing 10 000 small organic molecules (DiverSet, ChemBridge, San Diego, CA, USA); as described by Surpin *et al.* (2005). Briefly, each compound was dissolved in DMSO, diluted, and added to separate wells on a 24-well plate containing MS media agar. The chemicals were diluted to a final concentration of 50–100 μM. Approximately 12 sterilized *Arabidopsis* seeds were sown per well, stratified and grown vertically in the dark. Seven days after stratification, plates containing the seedlings were digitally photographed.

Images of all wells were screened for root phenotypes at the University of North Carolina at Chapel Hill. Candidate active compounds were identified and searches for analogues were done using the substructure search in the Hit2Lead database (Hit2Lead.com; Chembridge). Subsequent screens and dose–response curves were then performed with the corresponding compounds. From this, it was determined that the false positive rate of the primary screen was ~20%.

Root and hypocotyl elongation assays

Col-0 seeds were surface sterilized and then stratified in sterile water for 2 d at 4 °C in darkness. Approximately 15 seeds were sown into each well of a 12-well plate. Wells contained 1.5 ml 0.5× MS media+1% sucrose, pH 5.7. Chemical stocks (20 mM) were prepared from compounds that showed auxin-like activities. Aliquots of these stocks were added to the wells to obtain the desired final concentration. Plates were sealed with Parafilm (Pechiney Plastic Packaging, Chicago, IL, USA) and placed on a shaker (125 rpm) for a 5 d incubation period under white light (8 h) at 25 °C. Mild shaking provided even distribution and optimal uptake of the chemicals. Seedlings were fixed for at least 1 h in FAA (63% ethanol, 5% glacial acetic acid, 5% formaldehyde, water). Root and hypocotyl length were then captured using digital microscopy.

Assessment of hormone sensitivity

Dose–response curves of auxin-induced root growth inhibition were analysed by a non-linear regression to Weyers' equation (Weyers *et al.*, 1987; Weyers and Paterson, 1992):

$$R = R_{\text{Min}} + R_{\text{Amp}}([H]^P)/([H]^P + [H]_{50})$$

This function gives the response, R , to a given hormone concentration, $[H]$, where R_{Min} is equal to the growth rate in the

absence of hormone, R_{Amp} is equal to the maximal hormone-induced change, and $[H]_{50}$ is equal to the hormone concentration needed for a half maximal response. P describes possible deviations of the dose–response curves from a hyperbolic shape (ultrasensitive or subsensitive behaviour; see Guern, 1987). Since P did not significantly deviate from 1 in test runs of the fit, it was therefore fixed to 1 in all analyses. In some cases, the variability of R_{Amp} was limited to avoid gross negative R values (shrinkage) at high hormone concentrations.

Coleoptile growth (12 h assay)

Maize seeds, variety Silver Queen (Southern States Cooperative, Richmond, VA, USA) were rinsed with running tap water overnight and spread onto moist paper on a deep tray. The tray was covered with aluminium foil and the seeds were incubated at 30 °C for 4 d. Coleoptiles were harvested and the apical 3 mm removed. Subsequently, the coleoptiles were incubated in 0.5× MS medium+1% sucrose, pH 5.7, for 1 h with gentle shaking in order to remove the natural auxin source. Coleoptiles were transferred into new medium containing appropriate effector concentrations and incubated for 12 h (mild shaking). Coleoptile length was measured by means of a ruler. High resolution assays for instantaneous growth rates were performed as previously described (Lüthen *et al.*, 1990).

Auxin-inducible gene expression

Seeds from plants containing the *DR5::GUS* reporter (Ulmasov *et al.*, 1997) were subjected to the same treatment as plants grown for elongation assays. To examine auxin-regulated expression of the *DR5::GUS* reporter, GUS (β-glucuronidase) staining was performed following the method described by Malamy and Benfey (1997). Seedlings were transferred into staining solution containing X-GAL (5-bromo-4-chloro-3-indolyl-β-D-galactopyranoside) for detection of GUS activity and incubated at 37 °C overnight.

DR5rev::GFP-containing seeds were obtained from the Nottingham Arabidopsis Stock Centre (NASC ID: N9361). The seeds were stratified for 4 d at 4 °C on moist paper in sealed Petri dishes. Plants were then grown under white light for 16 h and etiolated for 2 d at the same temperature. At $t=0$, seedlings were carefully transferred into small Petri dishes (3–5 seedlings per Petri dish) containing 1.5 ml growth medium (10 mM KCl/1 mM CaCl₂). Images were captured using a Zeiss inverse IM 35 fluorescence microscope with excitation at 450–490 nm and emission band pass of 515–565 nm. The microscope was equipped with a Canon 350D camera. Images were converted from RAW-format to tiff using RAWDrop (version 1.04, written by Frank Siebert, 2004). Brightness of calibrated images was calculated using FITSwork (version 3.37, written by J Dierks, e-mail: jdierks.fw@freenet.de). See <http://astrosurf.com/buil/exoplanet/phot.htm> for photometric capabilities of DSLR cameras. After taking the first set of pictures, indicated compound concentrations were reached by adding a stock solution in DMSO. At $t=24$ h, a second set of pictures was taken to determine changes in fluorescence.

Genetic screens

EMS (ethylmethane sulphonate)-mutagenized seedlings were obtained from Lehle Seeds (Round Rock, TX, USA), surface sterilized, and stratified for 2 d in sterile water. A six-well plate format was used, and about 250 seeds were placed in each well. Seedlings were grown in 0.5× MS media with 1% sucrose at 20 nM WH7 ($[H]_{50}=9$ nM). Seedlings were also exposed to 30 nM WH9 ($[H]_{50}=34$ nM) and 30 nM WH13 ($[H]_{50}=27$ nM) individually in order to identify mutants resistant to these two compounds. Plants were incubated for 5 d at 24 °C before screening. The resistance of putative mutants was confirmed by growing the mutant seedlings in a 12-well plate format. Ten to fifteen seeds were sown per well, at

the indicated concentrations of compound. Seedlings were grown in $0.5\times$ MS media with 1% sucrose in a 24 °C growth chamber at 100 rpm.

Results

Screening of the DiverSet library for bioactive compounds

One of the well-known effects of auxin on plants is the inhibition of root growth at nanomolar concentrations. This physiological response was used to screen a library of 10 000 chemicals for compounds that have an auxin-like mode of action. Thirteen compounds were found to reproducibly and potently reduce root elongation and were designated WH1 to WH13 (Table 1). *Arabidopsis* seeds were exposed to various concentrations of the compounds selected from the DiverSet scan to obtain dose–response kinetics in a root growth inhibition assay. Because of its low $[H]_{50}$, WH7 was chosen to carry out a structure-similarity search in ChemMine (<http://bioweb.ucr.edu/ChemMineV2/>). Seven structure-informative acetamide analogues were chosen for further testing and designated WH7A to WH7G (Table 1). Also included were two structurally related compounds found in the primary screen: 2-(4-bromophenoxy)-*N*-(5-chloropyridin-2-yl)acetamide (WH11), which is identical to WH7A except for a bromo-substituent and 3-((2,4-dichlorophenoxy)methyl)-1*H*-1,2,4-triazole-5(4*H*)-thione (WH13), which contains a triazole-thione moiety.

Activity of 20 auxins identified in the screen

Although active auxins promote shoot growth at μ M concentrations, they specifically inhibit root elongation. The efficacy of the compounds tested is shown in Fig. 1. WH7 and the known auxins 2,4-D and 4-D exhibit a similar activity on root elongation (Fig. 1D), and their $[H]_{50}$ values are all in a range of 10–20 nM (Fig. 1A, B). WH7C, WH13, WH7A, and WH7G are amide derivatives of 2,4-D or WH7 (Fig. 1A, B). The exchange of the carboxylic acid against a *para*-substituted pyridine ring (WH7C) or a triazole-thione moiety (WH13) had no effect on efficacy. By contrast, the substitution in WH7G has a dramatic impact that increases the $[H]_{50}$ over 150-fold (Fig. 1A, E). It has to be considered that the potency depends on the tendency to undergo cleavage rather than the chemical properties of the amide groups (discussed below). WH7A is identical to WH7 with the exception of its amide substituent (Fig. 1B) and has similar activity (Fig. 1F). The absence of the methyl-group in 4-D entails no significant changes in auxin action. However, displacement of the methyl-group to the meta-position (WH7E) greatly reduced activity (Fig. 1B, F). The size and electronic density of the halogen substituent is critical. Replacement of chlorine with bromine or a methyl-group (Fig. 1C) decreases potency (Fig. 1G).

$[H]_{50}$ values in the root growth inhibition assay for a number of additional substances are shown in Table 1 including the commonly used auxins, IAA and NAA. The sequence of auxin activity according to the root growth inhibition assay is WH7 > 2,4-D \cong WH7C \cong WH7A > 4-D > WH13 > > WH11 > WH7E >> WH7D, WH7G. The value for IAA is probably an overestimate as it is most likely affected by strong metabolic decay during the 5 d of the assay. The fact that IAA is a very potent auxin on shorter timescales is evident from Fig. 3. The structure–activity relationship is discussed further below.

The definition of an auxin is a compound that promotes growth of etiolated cereal coleoptiles (Went, 1928). Therefore, the activity of the compounds was determined using the classical coleoptile growth assay. Dose–response curves for the growth response after 12 h (Fig. 2) demonstrate that both the amplitude of the stimulation and the $[H]_{50}$ values for the growth stimulation are structure-dependent. Higher concentrations of the classical auxins 2,4-D, IAA, and 4-D are inhibitory on elongation growth, resulting in bell-shaped dose–response curves (Fig. 2A), as do some of the new substances (e.g. WH13 and WH9; Fig. 2C). Interestingly, WH7 and its derivatives do not have a bell-shaped dose–response curve (Fig. 2B). Table 2 shows estimated or computed $[H]_{50}$ values for the inhibitory and stimulating components and the amplitudes. The sequences of activity for coleoptile growth stimulation are:

$[H]_{50}$: 2,4-D > WH13, 4-D, WH7 > WH7E, IAA > WH7G > WH7B > WH11 > WH7D >> WH3, WH9

amplitude: WH13 > 2,4-D, WH7 > IAA, WH7D > WH7B > WH7G > WH7E, 4-D >> WH11 >> WH3, WH9

For growth inhibition at higher concentrations the following pattern is found:

4-D > 2,4-D >> IAA, WH13

Dose–response curves of the other substances were not bell-shaped, thus there was no growth inhibition at higher concentrations.

Growth induction is a rapid response

Auxin-induced growth is a rapid process (Evans, 1974); therefore a transducer-based auxanometer was used to assess the activity of selected substances at a higher temporal resolution (Lüthen and Böttger, 1992). Figure 3 shows the time courses of growth responses induced by IAA, WH7, WH7E, and WH7G at various concentrations. WH7 and WH7E induce growth after a short lag phase with a time course similar to IAA. Compared with IAA, WH7 and WH7E induced a more sustained elongation response, probably because these substances have different transport and metabolic properties. This may also

Table 1. Structures of auxenic substances tested for this study with the $[H]_{50}$ values in the root growth inhibition assay

Stars indicate possible cleavage sites discussed in the text. Upper left: the natural auxin IAA and synthetic commercial auxins NAA, 2,4-D, and 4-D, followed by new auxin-like compounds. Upper right: less potent substances. Bottom: highly potent auxenic compound WH7 and analogues.

Compound	Structure	$[H]_{50}$	Compound	Structure	$[H]_{50}$
IAA $C_{10}H_9NO_2$		484 [nM]	5929059 WH1 $C_9H_{10}N_4O_2S$		4.1 [μ M]
NAA $C_{12}H_{10}O_2$		102 [nM]	6082970 WH2 $C_{23}H_{26}N_2O_2S$		21.7 [μ M]
2,4-D $C_8H_6Cl_2O_3$		12 [nM]	6075259 WH4 $C_{12}H_6Cl_4O_4S$		7.2 [μ M]
4-D $C_8H_7ClO_3$		19 [nM]	6160471 WH5 $C_{21}H_{21}N_3O_2$		6.6 [μ M]
6239040 WH13 $C_9H_7Cl_2N_3OS$		27 [nM]	6164585 WH6 $C_{18}H_{18}N_2O_3$		1.3 [μ M]
6212206 WH9 $C_{16}H_{16}ClN_3O_3$		34 [nM]	6162317 WH8 $C_{15}H_{16}FN_3O_4$		9.7 [μ M]
6191107 WH11 $C_{13}H_{10}BrClN_2O_2$		82 [nM]	6231481 WH10 $C_{14}H_{11}ClN_2O_3$		12.5 [μ M]
5120191 WH3 $C_{17}H_{19}NO_3$		1.8 [μ M]	6220480 WH12 $C_{19}H_{15}NO_5$		11 [μ M]
6156005 WH7 $C_{11}H_{11}ClN_4O_2$		9 [nM]	6071790 WH7D $C_{14}H_{12}BrClN_2O_2$		2.1 [μ M]
6215658 WH7A $C_{14}H_{12}Cl_2N_2O_2$		14.4 [nM]	6229098 WH7E $C_{14}H_{12}Cl_2N_2O_2$		101 [nM]
6201133 WH7B $C_{15}H_{15}ClN_2O_2$		870 [nM]	6056283 WH7F $C_{10}H_8Cl_2N_4OS$		> 1000 [nM]
5530074 WH7C $C_{13}H_9Cl_3N_2O_2$		13 [nM]	5809836 WH7G $C_{11}H_{14}ClNO_3$		2 [μ M]

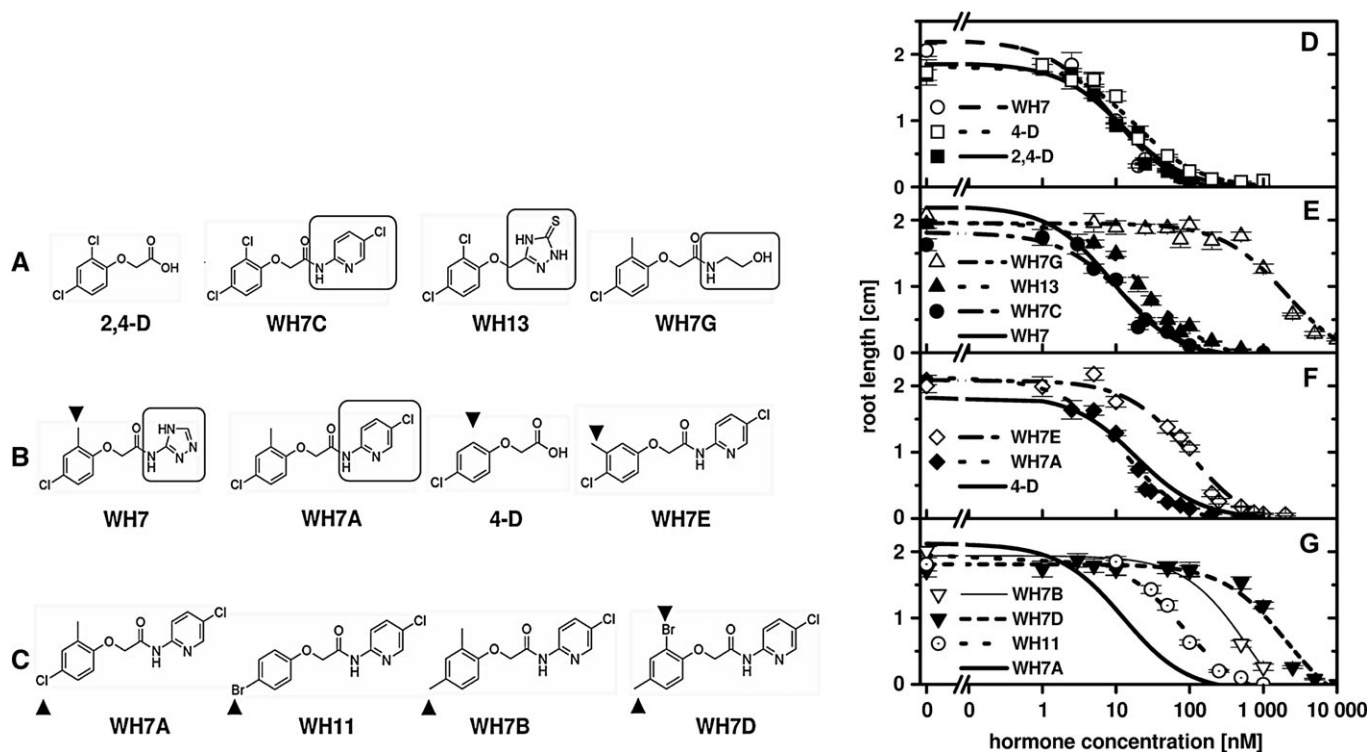


Fig. 1. Screening of the DiverSet library resulted in the identification of several auxin-active substances. (A), (B) and (C) show structures of the substances. Also given are $[H]_{50}$ values in the root growth inhibition assay, as well as the structures and activities of known auxins (2,4-D and 4-D). (D–G) Dose–response kinetics of WH7 analogues and related substances. Data points indicate means \pm SE of 25–50 individual measurements. Straight lines are function plots of Weyers' equation derived from a non-linear regression.

explain the poor performance of IAA in long-term root growth inhibition and coleoptile growth bioassays described above.

WH7 and WH13 are affected by the auxin influx carrier inhibitor 1-naphthoxyacetic acid (1-NOA)

Figure 4 shows that the transport of WH7 and WH13 shares properties with 2,4-D. The auxin influx carrier inhibitor 1-NOA was used as the diagnostic assay (Parry *et al.*, 2001). In line with previous reports, the dose–response curve for IAA was not significantly altered by 1-NOA treatment (data not shown).

Expression of auxin-induced genes by the compounds

To determine if the novel compounds act in an auxin-related signalling pathway, auxin-induced gene expression was analysed first using a *DR5::GUS* gene reporter system. Staining intensity and patterns induced by several auxins were compared (Fig. 5). The staining patterns differed between compounds (pictures not shown). Particularly noticeable is the good correlation between the intensity of GUS staining in the root–shoot junction and the activity rank of compounds in the physiological assays (compare $[H]_{50}$ values). Other plant hormones like abscisic

acid and cytokinin (kinetin, data not shown) had no effect on GUS expression.

Quantitative determination of the auxin-like response

Induction of GFP fluorescence, driven by activation of the synthetic auxin-responsive promoter *DR5*, could be used not only to determine the pattern of auxin response, but also to yield quantitative data (Saffarian *et al.*, 2007). Images of *DR5rev::GFP* plants were analysed at $t=0$ and after 24 h of chemical treatment by calculating the average brightness of pixels in a defined tissue area (e.g. root elongation zone) and subtraction of background. Brightness values and GFP-expression patterns were compared for the synthetic auxin 2,4-D as well as for WH7, WH7E, and WH7G. WH7 and analogues exhibited expression dynamics resembling those of known auxins (Fig. 6). Untreated *Arabidopsis* seedlings show a GFP-activity maximum in the root tip, correlating with maximal auxin accumulation in this tissue (Sabatini *et al.*, 1999). Increased fluorescence in the control at $t=24$ h reflects accumulation of GFP over time. After 24 h of treatment with 10^{-6} M, the maximum of fluorescence shifted into the root elongation zone. The activity follows the sequence: 2,4-D > WH7 > WH7E > WH7G and is consistent with their potency in the root growth inhibition and coleoptile growth assays.

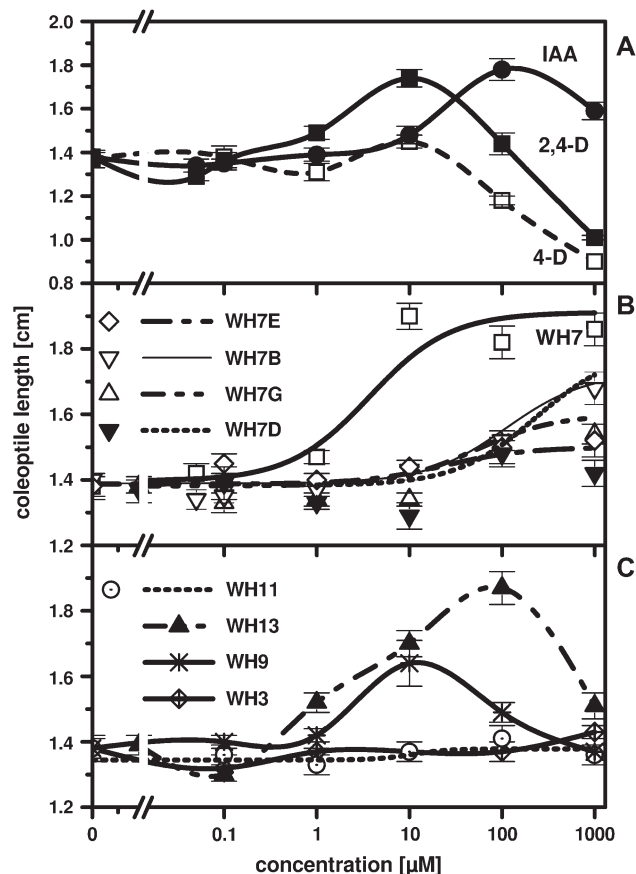


Fig. 2. Dose–response curves for several auxin-like substances in the maize coleoptile growth assay. (A) 2,4-D, 4-D, and IAA yield a bell-shaped dose–response curve. (B) Activity of WH7 and its derivatives. Note that the curves saturate. (C) Activity of some selected substances tested for this work. Data points indicate means \pm SE of 10–35 individual measurements. Straight lines are function plots of Weyers' equation derived from a non-linear regression (Fig. 3B) or splines in the case of the bell-shaped curves (Fig. 3A, C).

WH7-resistant mutants have an auxin-sensitive phenotype

Several auxin mutants have been identified using screens for resistance to growth inhibitory amounts of auxin. To determine if these newly identified compounds operate in a genetically defined auxin pathway, a pilot screen for mutations that confer resistance to them was performed. EMS-treated M2 seeds were screened for resistance to WH7, WH9, and WH13, based on primary root growth. These compounds were picked based on their potency and differences in substitutions at the phenoxy ring. Out of \sim 30 000 M2 individuals, nine putative resistant mutants were identified and subsequently confirmed segregating 3:1 resistance in the next generation, indicating the trait is dominant. Mutants designated *wh7-r1*, *wh7-r4*, *wh7-r6*, and *wh7-r7* were resistant to the inhibition of primary root elongation by WH7 (Fig. 7A). Several WH7-resistant mutants developed aerial rosettes (Fig. 8B), a phenotype associated with mutants of the auxin pathway gene

Table 2. $[H]_{50}$ values and amplitudes for the auxin effect of natural and synthetic auxins

Designation	$[H]_{50}$ stimulation	R_{Amp} stimulation	$[H]_{50}$ inhibition	R_{Amp} inhibition
IAA	50*	0.43*	1000*	-0.6*
2,4-D	1.4*	0.5*	136*	-0.6*
4-D	3.5	0.1*	100*	-0.6*
WH13	2*	0.6*	1000*	-0.6*
WH7	3.7	0.5	–	–
WH7G	51.1	0.21	–	–
WH7E	23.7	0.11	–	–
WH7D	233	0.42	–	–
WH7B	111.8	0.33	–	–
WH11	215.7	0.03	–	–
WH3	–	–	–	–
WH9	–	–	–	–

* Values estimated from graphs; all other values were taken from fits to Weyers' equation. Substances listed without values did not show significant activity with regard to the relevant parameter. For bell-shaped dose–response curves $[H]_{50}$ values and amplitude values for the inhibitory branch of the curve are also given. Chi-square values for all fits are 0.001 or smaller.

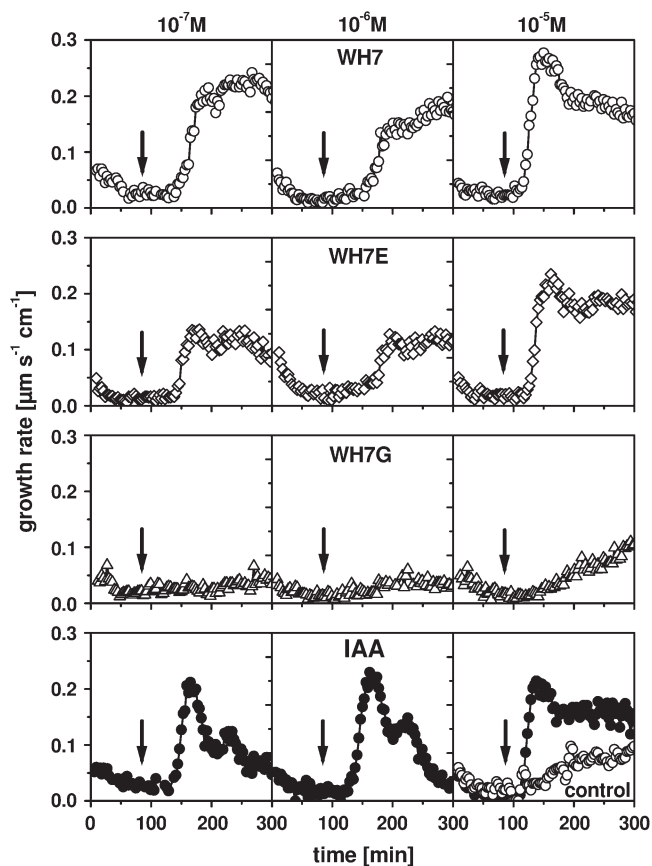


Fig. 3. Time courses of growth responses induced in maize coleoptiles by WH7, WH7E, WH7G, and IAA (from top to bottom), as measured with an angular transducer. The substances were applied at the time indicated by the arrows. The control shows the typical onset of elongation growth after a few hours caused by restoration of internal auxin production. Data points indicate the growth rate of five stacked coleoptiles, measured simultaneously. Typical results are shown.

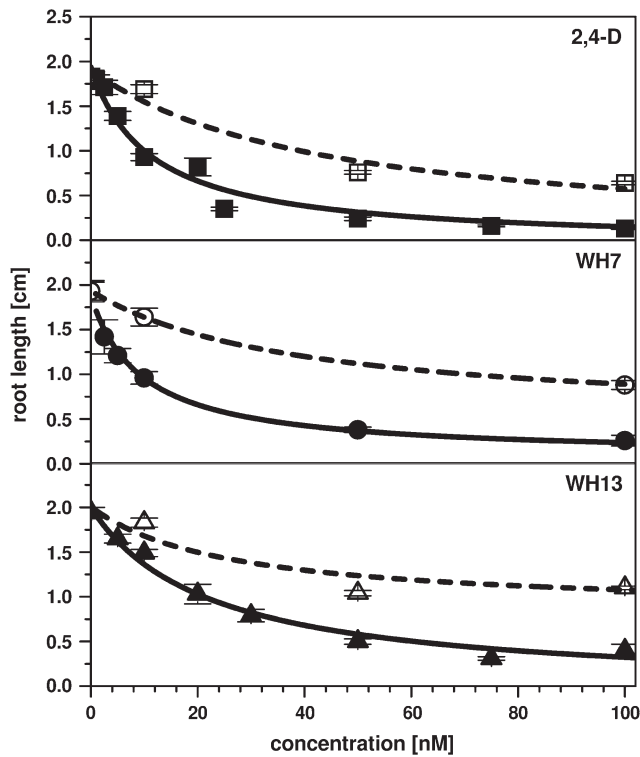


Fig. 4. Dose–response curves of root growth inhibition by 2,4-D, WH7, and WH13 (closed symbols). Open symbols show the result in the presence of the auxin influx carrier inhibitor 1-NOA (10 μ M). Data points indicate means \pm SE of a minimum of 15 individual measurements. Lines are function plots of Weyers' equation derived from a non-linear regression.

CAND1 (Cheng *et al.*, 2004). As a number of WH7-resistant mutants developed aerial rosettes, *cand1-1* mutants were tested for WH7 resistance. Figure 7C displays the dose-dependent response of *cand1-1* to WH7. 2,4-D was used as a positive control. Relative to wild-type, the *cand1-1* mutant shows less inhibition of primary root development when exposed to WH7 and 2,4-D. These results suggest that WH7 behaves in a manner similar to 2,4-D and that WH7 can signal in the *CAND1* pathway.

Mutant *wh7-r1* was characterized further. F2 from a *wh7-r1* backcross to Col-0 yielded 92% of the offspring resistant to WH7, indicating that *wh7-r1* was homozygous for a dominant mutation. Because this cross was made into a wild-type plant, it is possible that the carpel was contaminated by wild-type pollen, accounting for the 8% discrepancy. The dominance of this mutation is noteworthy because there are known dominant auxin mutants; in particular, several dominant mutations in the AUX/IAA repressor proteins have been characterized (Nagpal *et al.*, 2000; Woodward and Bartel, 2005).

Discussion

Auxin activity of novel substances

It was concluded that WH7 and analogues described here are active auxins in a number of classical physiological assays. They promote growth in coleoptiles (Figs 2, 3),

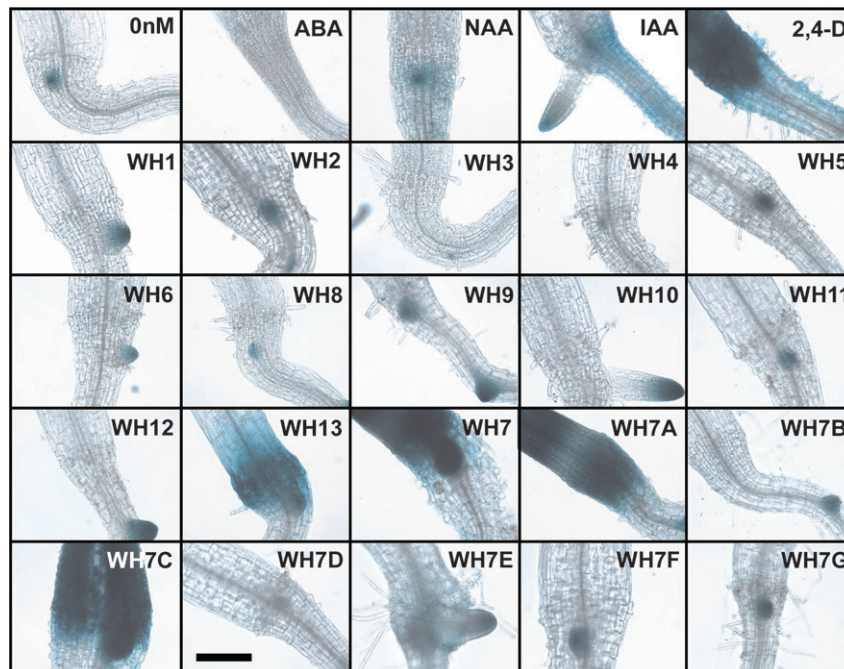


Fig. 5. Expression patterns of the *DR5::GUS* reporter in the root–shoot junction of plants treated with auxins and other small organic molecules eliciting auxin-like growth effects in *Arabidopsis* roots and shoots. Effector concentration = 50 nM. Reporter expression is indicated by blue staining. GUS activity is highest in 2,4-D, WH7, WH7A, and WH7C, followed by WH13 and IAA. Scale bar = 100 μ m.

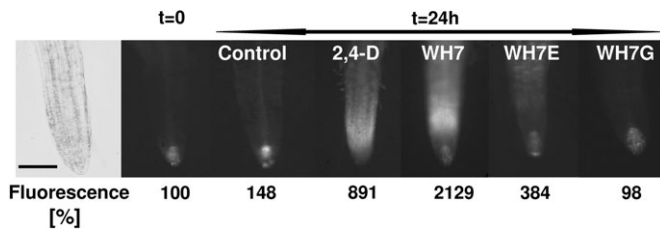


Fig. 6. Time-dependent GFP-expression profile induced by auxin and related chemicals. From left to right: *Arabidopsis* root tip and elongation zone (bright field); GFP fluorescence in the same plant section (base level of $t=0$ was set to 100%); control showing base level after 24 h; fluorescence induced by 2,4-D, WH7, WH7E, and WH7G (10^{-6} M) after 24 h. Fluorescence intensity data indicate means of three individual experiments. Measurements were carried out framing a section of $25\ \mu\text{m} \times 50\ \mu\text{m}$ in the elongation zone, $\sim 100\ \mu\text{m}$ distant from the root tip. Scale bar = $100\ \mu\text{m}$.

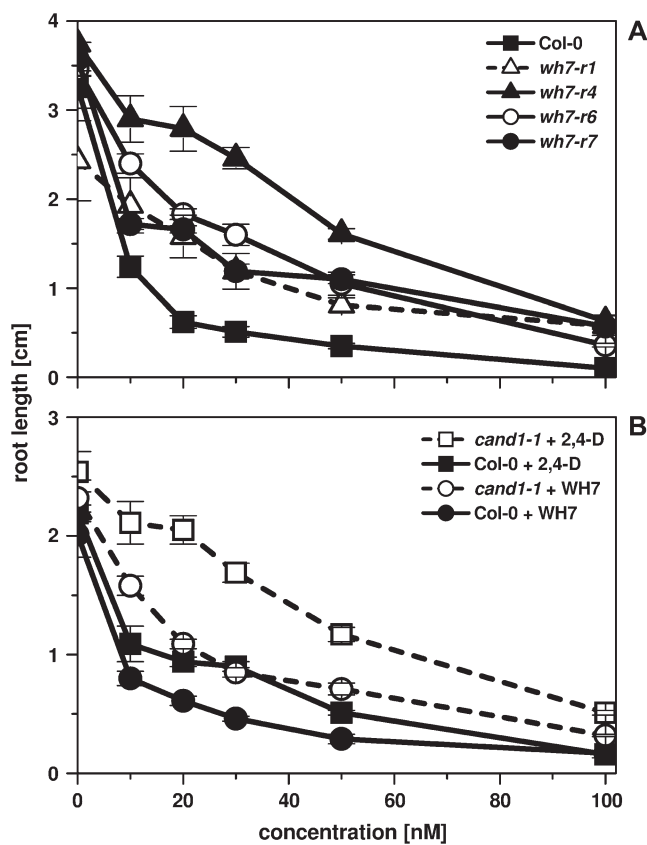


Fig. 7. Dose-response kinetics of mutants resistant to primary root growth inhibition elicited by WH7 and 2,4-D, respectively. (A) Four mutant lines, designated *wh7-r1*, *wh7-r4*, *wh7-rb*, and *wh7-r7*, were identified in a screen for mutations that confer resistance to WH7. (B) The *cand1-1* mutant (open symbols) is resistant to both WH7 and 2,4-D. Data indicate means \pm SE of five to nine individual measurements.

inhibit root elongation (Figs 1, 4, Table 1), and activate a synthetic auxin promoter (Figs 5, 6). The amplitude or $[H]_{50}$ value depended strongly on the backbone substitutions (discussed further below). WH7, WH7C, WH7A, and WH13 are highly potent auxins, comparable in

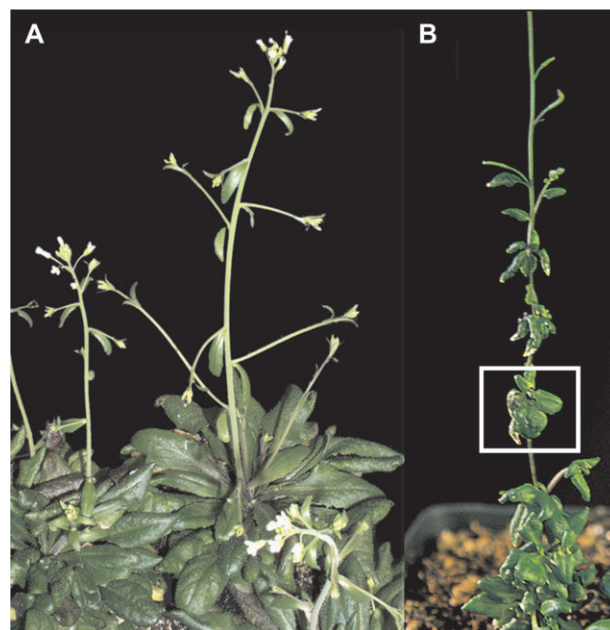


Fig. 8. (A) *Arabidopsis thaliana* wild-type (Col-0). (B) The WH7-resistant mutant *wh7-r1* develops aerial rosettes (see box). Aerial rosettes are a distinct phenotype associated with *cand1* mutants.

activity to 2,4-D and 4-D. The inhibitory action on coleoptile growth at supraoptimal concentrations, resulting in bell-shaped dose-response curves, was not detected in many of the substances.

Possible cleavage of some amide auxins

Possible cleavage *in vivo* must be considered when describing new auxins (Dai *et al.*, 2005). Like esters, amides are lipophilic and may readily enter the cell by passive diffusion. Once inside the cell, they may be cleaved by amidases (or other enzymes like carboxypeptidases), which will convert them to free acids (Jones *et al.*, 1949; Fawcett *et al.*, 1958; Evans and Rayle, 1970). The partial double bond character of the amide bond can be strengthened or weakened by modifications that favour one resonance form over another. Donating a hydrogen bond to amide nitrogen should favour the single-bonded, less stable form. Similarly, a strongly electronegative substituent (such as chlorine) near the amide nitrogen favours the single-bonded form by competing with the amide oxygen to 'steal' an electron from the amide nitrogen. According to this rationale WH3 (Table 1), WH7, WH7A, and derivatives (Fig. 1) are likely to be hydrolysed. WH7 and its derivative WH7A would yield MCPA (4-chloro-2-methylphenoxyacetic acid). 4-Chlorophenoxyacetic acid reportedly has auxin activity, while the activity of 2-methylphenoxyacetic acid is quite weak (Katekar, 1978). A shift of the methyl-group from 2- into 3- position, as in WH7E, resulted in a considerable drop in activity. Cleavage of WH7G is less likely, which may

explain its low potency in all assays. Upon cleavage, WH3 and WH7B would become 2,4-dimethylphenoxyacetic acid, which has auxin activity in the pea split test (Katekar, 1978). Only the exchange of the *para*-substituted pyridine ring of WH7B against an anisole group in WH3 entails changes that affect the molecules capacity to undergo cleavage. One would predict that the amide bond in WH7B is less stable than in WH3 and this corresponds very well with the $[H]_{50}$ values of 870 nM and 1800 nM, respectively. WH13 could be cleaved to 2,4-D. It appears, however, unlikely that this is the only mechanism contributing to its activity, as it has a much higher $[H]_{50}$ value than 2,4-D alone. When cleaved, WH5 resembles 2-naphthoxyacetic acid (2-NOA), which has auxin activity, but is also a known auxin influx inhibitor (Parry *et al.*, 2001; Hössel *et al.*, 2005).

It has to be additionally considered that the substitutions not only affect the stability of the amide bond, but also change the interaction of the molecules with the catalytic site of the amidases and/or a target protein.

Auxin action of amides requires active transport into the cell

Amides typically are regarded as compounds with low water solubility. They are significantly less water soluble than comparable acids or alcohols due to their non-ionic character, the presence of non-polar hydrocarbon functionality, and the inability of tertiary amides to donate hydrogen bonds to water (they can only be H-bond acceptors). Thus amides have water solubility roughly comparable to esters. Amides are also less soluble than comparable carboxylic acids since these compounds can both donate and accept hydrogen bonds and can ionize at appropriate pH to further enhance solubility. From this, easy passage of the plasma membrane without facilitation is expected. However, the present data show that the auxin uptake inhibitor 1-NOA (Yang *et al.*, 2006) reduces the sensitivity to WH7 (Fig. 5B) and WH13 (Fig. 5C). 1-NOA has been shown to reduce the sensitivity to 2,4-D (Parry *et al.*, 2001), but not to IAA—an observation confirmed here (Fig. 5A, data for IAA not shown). This was explained by the hypothesis that 2,4-D, but not IAA, requires active uptake by AUX1 and LAX influx carriers (Ottensschläger *et al.*, 2003). If this interpretation is correct one would expect that WH7 and WH13 are both actively transported into the cell. This would also suggest that diffusion and subsequent intracellular cleavage, as described above, play a minor role in WH13 and WH7 action. An alternative interpretation is that WH7 and WH13 are taken up passively and are subsequently cleaved. The resulting acidic form may be exported by the auxin efflux carrier system. Their re-import into the next cell layer may then involve influx carriers, which explains the inhibitory effect of 1-NOA.

Structure–activity relationships of the substances

Katekar (1978) postulated that auxin-binding involves at least two different areas of interactions: (i) the carboxyl acceptor, non-covalently binding to the carboxylic group of IAA, and (ii) the acceptor site for aromatic ring structures. As described above, the amides may be converted to carboxylic groups upon uptake. For WH7 and its analogues, the position of the carboxylic or amide group is identical; therefore, the observed differences in activity depend on structural requisites of the aromatic ring system. The sole exception is WH7G (Fig. 1A), which is not likely to be cleaved and therefore is not effective.

The aromatic ring system and substitution requisites

WH7, WH7A, WH7C, WH9, and WH13, with $[H]_{50}$ values between 9 nM and 27 nM, were among the most potent compounds found in the root elongation assay (Fig. 1). Like 2,4-D, the structures of WH7C and WH13 include a phenoxy group with two chlorine substituents on the aromatic ring (Fig. 1A). For the ortho-position, replacement of the ortho-chlorine on the phenoxy ring against a methyl-group (WH7 and WH7A; Fig. 1B) had no effect. Even complete removal of the group, as represented by 4-D, had no strong influence on capacity. Displacement as in WH7E, however, caused a 10-fold increase in $[H]_{50}$ (Fig. 1B). For the *para*-position, bromine, another halogen with a slightly wider radius, could replace chlorine without completely abolishing activity of the compound (WH11; Fig. 1C). By contrast, replacement with a methyl-group resulted in considerable drop in activity (seen in WH7B; Fig. 1C), which is exceeded when the bromine is moved to the ortho-position (WH7D).

WH7, WH7E, and WH7G show a similar structure–activity relationship in monocots and dicots

2,4-D is a selective herbicide causing growth disorders in dicots, but not in monocots. It has been speculated that this selective lethality is caused by two amino acid substitutions in the auxin-binding site of ABP1 (Woo *et al.*, 2002). It has been known for a long time that 2,4-D is a strong auxin in coleoptile growth tests as well as in dicot hypocotyl elongation. In the present study, WH7 and its derivatives, 2,4-D and 4-D, display a similar sequence of activity in *Arabidopsis* root growth inhibition and in the maize coleoptile growth test. The order of potency in maize followed a very similar profile in the dicot plant *Arabidopsis* (2,4-D = WH7 > WH7E > WH7G).

WH7 action can be genetically defined

The isolation of mutants, altered in hormone response, has been a powerful approach to understand the mechanism of

auxin action. Detailed physiological studies of auxin-resistant mutants revealed important information about the wild-type function of the mutated genes and the mechanism of auxin action. Since the isolation of auxin-related mutants has been used, major players involved in every aspect of auxin-signal transduction have been identified (reviewed in Leyser, 1997). Recent screens for mutants resistant to sirtinol, a synthetic molecule activating auxin transduction (Dai *et al.*, 2005), uncovered the role of the auxin response factors ARF19 and ARF7 in auxin and ethylene signalling (Li *et al.*, 2006). A genetic screen for mutants insensitive to sirtinol also resulted in the discovery of *cand1-1*. CAND1 has been shown to be involved in the regulation of the SCF complex, which is a part of the protein degradation machinery (Cheng *et al.*, 2004; Feng *et al.*, 2004).

In this study, the action of novel synthetic auxin-like substances was carefully characterized. It was found that these compounds act in a physiologically relevant concentration range. The sequence of activity was consistent throughout all assays and plant species. A good correlation was also found between auxin-related gene expression, as indicated by GUS staining and induction of GFP fluorescence, and *in vivo* activity. These novel substances complement the array of tools available for auxin researchers. Currently, the characterization of putative auxin receptors is among the major topics. The use of structurally distinct auxins will help to distinguish between auxin sensors and to dissect related pathways.

Supplementary data

IUPAC designations of the substances tested in this study are provided as supplementary material in Table S1 and can be found on *JXB* online.

Acknowledgements

We are extremely grateful to Dr Natasha Raikhel, University of California at Riverside, for sharing unpublished data that made this work entirely possible. We thank Dr Terrence A. Walsh (Dow Agrosciences, Indianapolis, IN, USA) for helpful suggestions. We also greatly acknowledge the technical assistance of Jin Yang and Cathy Jones. This study was supported by a Feodor Lynen grant from the Humboldt foundation through a fellowship to MC and by grants from NIGMS (R01GM065989), DOE (DE-FG02-05er15671) and NSF (MCB-0209711) to AMJ.

References

Armstrong JI, Yuan S, Dale JM, Tanner VN, Theologis A. 2004. Identification of inhibitors of auxin transcriptional activation by means of chemical genetics in *Arabidopsis*. *Proceedings of the National Academy of Sciences, USA* **101**, 14978–14983.

- Barbier-Brygoo H, Ephritikhine G, Klämbt D, Maurel C, Palme K, Schell J, Guern J. 1991. Perception of the auxin signal at the plasma membrane of tobacco mesophyll protoplasts. *The Plant Journal* **1**, 83–93.
- Chen JG, Shimomura S, Sitbon F, Sandberg G, Jones AM. 2001a. Role of auxin-binding protein 1 in leaf cell growth. *The Plant Journal* **28**, 607–617.
- Chen JG, Ullah H, Young JC, Sussmann MR, Jones AM. 2001b. ABP1 is required for organized cell elongation and division in *Arabidopsis* embryogenesis. *Genes & Development* **15**, 902–911.
- Cheng Y, Dai X, Zhao Y. 2004. AtCAND1, a HEAT-Repeat protein that participates in auxin signaling in *Arabidopsis*. *Plant Physiology* **135**, 1020–1026.
- Christian M, Steffens B, Schenck D, Burmester S, Böttger M, Lüthen H. 2006. How does auxin enhance cell elongation? Role of auxin-binding proteins and potassium channels in growth control. *Plant Biology* **8**, 346–352.
- Christian M, Steffens B, Schenck D, Lüthen H. 2003. The *diageotropica* mutation of tomato disrupts a signaling chain using extracellular auxin binding protein 1 as a receptor. *Planta* **218**, 309–314.
- Claussen M, Lüthen H, Böttger M. 1996. Inside or outside? Localization of the auxin receptor relevant to auxin-induced growth. *Physiologia Plantarum* **98**, 861–867.
- Dai X, Hayashi K-I, Nozaki H, Cheng Y, Zhao Y. 2005. Genetic and chemical analyses of the action mechanisms of sirtinol in *Arabidopsis*. *Proceedings of the National Academy of Sciences, USA* **102**, 3129–3134.
- Dharmasiri N, Dharmasiri S, Estelle M. 2005. The F-box protein TIR1 is an auxin receptor. *Nature* **435**, 441–445.
- Diekmann W, Venis MA, Robinson DG. 1995. Auxins induce clustering of the auxin-binding protein at the surface of maize coleoptile protoplasts. *Proceedings of the National Academy of Sciences, USA* **92**, 3425–3429.
- Evans ML. 1974. Rapid responses to plant hormones. *Annual Review of Plant Physiology* **25**, 195–223.
- Evans ML. 1984. Functions of hormones at the cellular level of organization. In: Pirson A, Zimmermann MH, eds. *Encyclopedia of plant physiology*, Vol. 10. Berlin: Springer Verlag, 23–79.
- Evans ML, Rayle DL. 1970. The timing of growth promotion and conversion to indole-3-acetic acid for auxin precursors. *Plant Physiology* **45**, 240–243.
- Fawcett CH, Taylor HF, Wain RL, Wightman F. 1958. The metabolism of certain acids, amides and nitriles within plant tissues. *Proceedings of the Royal Society of London, Biological Sciences* **148**, 543–570.
- Feng S, Shen Y, Sullivan JA, Rubio V, Xiong Y, Sun T-p, Deng XW. 2004. *Arabidopsis* CAND1, an unmodified CUL1-interacting protein, is involved in multiple developmental pathways controlled by ubiquitin/proteasome-mediated protein degradation. *The Plant Cell* **16**, 1870–1882.
- Guern J. 1987. Regulation from within: the hormone dilemma. *Annals of Botany* **60**, Suppl. 4, 75–102.
- Henderson J, Baully JM, Ashford DA, Oliver SC, Hawes CR, Lazarus CM, Venis MA, Napier RM. 1997. Retention of maize auxin-binding protein in the endoplasmic reticulum: quantifying escape and the role of auxin. *Planta* **202**, 313–323.
- Harnden D, Jones AM. 1995. Organ distribution of auxin-binding protein 1 in the etiolated maize seedling. *Journal of Plant Growth Regulation* **14**, 109–113.
- Hertel R. 1995. Auxin binding protein is a red herring. *Journal of Experimental Botany* **46**, 461–462.
- Hertel R, Thompson K-S, Russo VEA. 1972. *In vitro* auxin binding to particulate cell fractions from corn coleoptiles. *Planta* **107**, 325–340.

- Hössel D, Schmeiser C, Hertel R. 2005. Specificity patterns indicate that auxin exporters and receptors are the same proteins. *Plant Biology* **7**, 41–48.
- Jones AM, Herman E. 1993. KDEL-containing, auxin-binding protein is secreted to the plasma membrane and cell wall. *Plant Physiology* **101**, 595–606.
- Jones AM, Im KH, Savka MA, Wu MJ, DeWitt NG, Shillito R, Binns AN. 1998. Auxin-dependent cell expansion mediated by overexpressed auxin-binding protein 1. *Science* **282**, 1114–1117.
- Jones RL, Metcalfe TP, Sexton WA. 1949. The relationship between the constitution and the effect of chemical compounds on plant growth. *Biochemical Journal* **45**, 143–149.
- Katekar GF. 1978. Auxins: on the nature of the receptor site and molecular requirements for auxin activity. *Phytochemistry* **18**, 223–233.
- Kepinski S, Leyser O. 2005. The *Arabidopsis* F-box protein TIR1 is an auxin receptor. *Nature* **435**, 446–451.
- Kim Y-S, Min J-K, Kim D, Jung J. 2001. A soluble auxin binding protein, ABP57: purification with anti-bovine serum albumin antibody and characterization of its mechanistic role in auxin effect on plant plasma membrane H⁺-ATPase. *Journal of Biological Chemistry* **276**, 10730–10736.
- Klämbt D. 1990. A view about the function of the auxin-binding proteins at the plasma membrane. *Plant Molecular Biology* **14**, 1045–1050.
- Leyser O. 1997. Auxin: lessons from a mutant weed. *Physiologia Plantarum* **100**, 407–414.
- Li J, Dai X, Zhao Y. 2006. A role for auxin response factor 19 in auxin and ethylene signalling in *Arabidopsis*. *Plant Physiology* **140**, 899–908.
- Lipinski C, Hopkins A. 2004. Navigating chemical spaces for biology and medicine. *Nature* **432**, 855–861.
- Lüthen H, Bigdon M, Böttger M. 1990. Re-examination of the acid growth theory of auxin action. *Plant Physiology* **93**, 993–939.
- Lüthen H, Böttger M. 1992. A high-tech low-cost auxanometer for high resolution determination of elongation rates in six independent experimental setups. *Mitteilungen des Instituts für Allgemeine Botanik Hamburg* **24**, 13–22.
- MacBeath G. 2001. Chemical genomics: what will it take and who gets to play? *Genome Biology* **2**, 10.1186/gb-2001-2-6-comment2005.
- MacDonald H. 1997. Auxin perception and signal transduction. *Physiologia Plantarum* **100**, 423–430.
- Malamy JE, Benfey PN. 1997. Organization and cell differentiation in lateral roots of *Arabidopsis thaliana*. *Development* **124**, 33–44.
- Nagpal P, Walker LM, Young JC, Sonawala A, Timpote C, Estelle M, Reed JW. 2000. AXR2 encodes a member of the Aux/IAA protein family. *Plant Physiology* **123**, 563–574.
- Ottenschläger I, Wolff P, Wolverton C, Bhalerao RP, Sandberg G, Ishikawa H, Evans ML, Palme K. 2003. Gravity-regulated differential auxin transport from columella to lateral root cap cells. *Proceedings of the National Academy of Sciences, USA* **100**, 2987–2791.
- Parry G, Delbarre A, Marchant A, Swarup R, Napier R, Perrot-Rechenmann, Bennett MJ. 2001. Novel auxin transport inhibitors phenocopy the auxin influx carrier mutation *aux1*. *The Plant Journal* **25**, 399–406.
- Raikhel N, Pirrung M. 2005. Adding precision tools to the plant biologists' toolbox with chemical genomics. *Plant Physiology* **138**, 563–564.
- Sabatini S, Beis D, Wolkenfelt H, Murfett J, Guilfoyle T, Malamy J, Benfey P, Leyser O, Bechtold N, Weisbeeki P, Scheres B. 1999. An auxin-dependent distal organizer of pattern and polarity in the *Arabidopsis* root. *Cell* **99**, 463–472.
- Saffarian S, Li Y, Elson EL, Pike LJ. 2007. Oligomerization of the EGF receptor investigated by live cell fluorescence intensity distribution analysis. *Biophysical Journal* **93**, 1021–1031.
- Steffens B, Feckler C, Palme K, Christian M, Böttger M, Lüthen H. 2001. The auxin signal for protoplast swelling is perceived by extracellular ABP1. *The Plant Journal* **27**, 591–599.
- Surpin M, Rojas-Pierce M, Carter C, Hicks GR, Vasquez J, Raikhel NV. 2005. The power of chemical genomics to study the link between endomembrane system components and the gravitropic response. *Proceedings of the National Academy of Sciences, USA* **102**, 4902–4907.
- Tan X, Calderon-Villalobos LIA, Sharon M, Zheng C, Robinson CV, Estelle M, Zheng N. 2007. Mechanism of auxin perception by the TIR1 ubiquitin ligase. *Nature* **446**, 640–645.
- Tian H, Klämbt D, Jones AM. 1995. Auxin-binding protein 1 does not bind auxin within the endoplasmic reticulum despite this being the predominant subcellular location for this hormone receptor. *Journal of Biological Chemistry* **270**, 26962–26969.
- Ulmasov T, Murfett J, Hagen G, Guilfoyle TJ. 1997. Aux/IAA proteins repress expression of reporter genes containing natural and highly active synthetic auxin response elements. *The Plant Cell* **9**, 1963–1971.
- Walsh TA, Neal R, Merlo AO, Honma M, Hicks GR, Wolff K, Matsumura W, Davies JP. 2006. Mutations in an auxin receptor homolog AFB5 and in SGT1b confer resistance to synthetic picolinate auxins and not to 2,4-dichlorophenoxyacetic acid or indole-3-acetic acid in *Arabidopsis*. *Plant Physiology* **142**, 542–552.
- Went FW. 1928. Wuchsstoff und Wachstum. *Recueil des Travaux Botaniques Néerland* **25**, 1–116.
- Weyers JDB, Paterson NW. 1992. Quantitative assessment of hormone sensitivity changes with reference to stomatal responses to abscisic acid. In: Karssen CM, Van Loon LC, Vreugdenhil D, eds. *Progress in plant growth regulation*. Dordrecht: Kluwer Academic Publishers, 226–236.
- Weyers JDB, Paterson NW, A'Brook R. 1987. Towards a quantitative definition of plant hormone sensitivity. *Plant, Cell and Environment* **10**, 1–10.
- Woo EJ, Marshall J, Baulry J, Chen JG, Venis M, Napier RM, Pickersgill RW. 2002. Crystal structure of auxin binding protein 1 in complex with auxin. *EMBO Journal* **21**, 2877–2885.
- Woodward AW, Bartel B. 2005. Auxin: regulation, action, and interaction. *Annals of Botany* **95**, 707–735.
- Yamagami M, Haga K, Napier RM, Iino M. 2004. Two distinct signaling pathways participate in auxin-induced swelling of pea epidermal protoplasts. *Plant Physiology* **134**, 735–747.
- Yang Y, Hammes UZ, Taylor CG, Schachtmann DP, Nielsen E. 2006. High-affinity auxin transport by the AUX1 influx carrier protein. *Current Biology* **16**, 1–5.